Formation Mechanism and Low-Temperature Instability of Exciton Rings

L. V. Butov,[1,2] L. S. Levitov,[3] A. V. Mintsev,[1] B. D. Simons,[4] A. C. Gossard,[5] and D. S. Chemla[1,6]

[1]*Materials Sciences Division, E. O. Lawrence Berkeley National Laboratory, Berkeley, California 94720, USA*
[2]*Department of Physics, University of California San Diego, La Jolla, California 92093-0319, USA*
[3]*Department of Physics, Center for Materials Sciences & Engineering, Massachusetts Institute of Technology, 77 Massachusetts Avenue, Cambridge, Massachusetts 02139, USA*
[4]*Cavendish Laboratory, Madingley Road, Cambridge CB3 OHE, United Kingdom*
[5]*Department of Electrical and Computer Engineering, University of California, Santa Barbara, California 93106, USA*
[6]*Department of Physics, University of California at Berkeley, Berkeley, California 94720, USA*

(Received 6 August 2003; published 18 March 2004)

The macroscopic rings observed in the photoluminescence patterns of excitons in coupled quantum wells are explained by a mechanism of carrier imbalance, transport, and recombination. The rings originate from the spatial separation of p and n carriers, and occur at the interface of the p and n domains, where excitons are generated. We explore the states of excitons in the ring over a range of temperatures down to 380 mK and report a transition of the ring into a periodic array of aggregates, a new low-temperature ordered exciton state.

DOI: 10.1103/PhysRevLett.92.117404 PACS numbers: 78.55.Cr, 71.35.–y, 72.20.–i

Bound electron-hole pairs, excitons, are light Bose particles with a mass comparable to that of the free electron [1]. High quantum degeneracy temperatures and the possibility to control density by laser photoexcitation makes cold excitons a paradigm system for studies of collective states and many-body phenomena. As well as Bose-Einstein condensation [1], the cold exciton and electron-hole systems are expected to host a range of novel collective states, such as a BCS-like condensate [2], a paired Laughlin liquid [3], coupled Wigner solids [3], and an excitonic charge density wave [4].

The theoretical predictions above rely on the experimental realization of cold exciton gases. Although the semiconductor crystal lattice can be routinely cooled to temperatures well below 1 K in He refrigerators, after decades of effort with various materials, it appears to be experimentally challenging to lower the temperature of the exciton gas to even a few degrees kelvin. The exciton temperature, T_X, determined by the ratio of the energy relaxation and recombination rates, exceeds by far the lattice temperature in most semiconductors. For T_X to approach the lattice temperature, the lifetime of excitons should considerably exceed their energy relaxation time.

Because of the long lifetime and high cooling rate, the indirect excitons in coupled quantum wells (CQWs) form a unique system in which a cold exciton gas can be created. The long lifetimes are due to spatial separation of the electron and hole wells [5] while high cooling rates result from momentum conservation being relaxed in the direction perpendicular to the QW plane [6]. The repulsive interaction between indirect excitons stabilizes the exciton state against the formation of metallic electron-hole droplets [3,7] and results in screening of in-plane disorder [8].

The seemingly unique opportunity to realize a cold exciton gas has led to active experimental studies [9–17]. Recently, an intriguing observation was made of bright macroscopic exciton rings in the spatial photoluminescence (PL) patterns in CQWs with an onset of fragmentation of the external ring into an ordered array of aggregates taking place at a few degrees kelvin [15]. Luminescence rings were also observed in other CQW materials [17]. Yet neither the rings nor their fragmentation have been accounted for by theory.

Here, the conundrum of ring formation is resolved by new experiments, leading to a consistent and compelling picture based on the mechanism of carrier spatial separation and recombination at the interfaces of the p and n domains. We propose that, since the carriers binding to form the excitons are in thermal equilibrium with the lattice, the rings represent a source of cold excitons and, as such, present a new opportunity to study novel states of the cold exciton gas. With this motivation, we have explored states of excitons in the ring over a range of temperatures down to 380 mK and observed a sharp transition via modulational instability, giving rise to ring fragmentation into spatially ordered aggregates.

The measurements reported here were obtained from a molecular-beam-epitaxy –grown, electric-field-tunable n^+-i-n^+ GaAs/AlGaAs CQW structure [13,15]. The i region consists of two 8 nm GaAs QWs separated by a 4 nm $Al_{0.33}Ga_{0.67}As$ barrier and surrounded by 200 nm $Al_{0.33}Ga_{0.67}As$ barrier layers. The n^+ layers are Si-doped GaAs with $N_{Si} = 5 \times 10^{17}$ cm^{-3}. The electric field across the structure is monitored by the external gate voltage V_g applied between the highly conducting n^+ layers. For $V_g \gtrsim 0.3$ V the ground state is an indirect exciton [Fig. 1(d)] with a lifetime of ca. 10 – 100 ns [13]. The PL linewidth of about 1 meV indicates small in-plane disorder. The excitation was produced by a He Ne laser with a photon energy of 1.96 eV above $Al_{0.33}Ga_{0.67}As$ gap. The experiments were performed in ^{3}He and ^{4}He

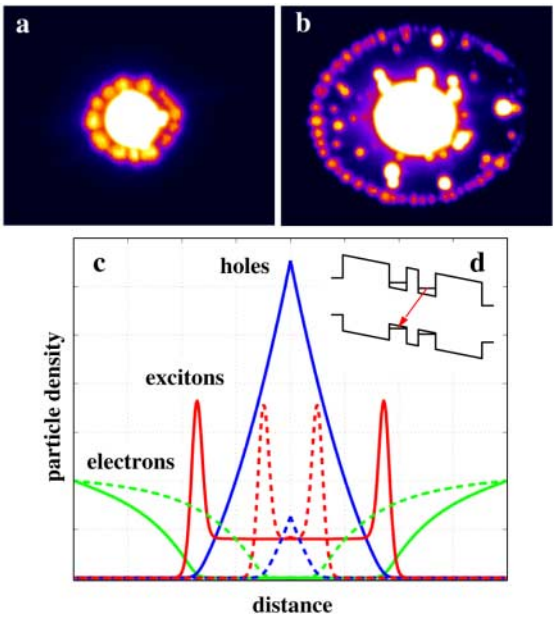

FIG. 1 (color online). Exciton rings at different photoexcitation intensity: The pattern of indirect exciton PL at $T = 380$ mK and $V_g = 1.24$ V for (a) $P_{ex} = 310$ μW and (b) $P_{ex} = 930$ μW. The excitation spot size is ca. 30 μm. The area of view is 410×330 μm. (c) The carrier distribution as predicted by the transport model, Eq. (1), at two excitation intensities (the scales are in a.u.). (d) The CQW band diagram.

cryostats with windows. The spatial pattern of the indirect or direct exciton PL was detected by charge-coupled device camera, with spectral selection made possible by the interference filter adjusted to the exciton emission energy. The spatial resolution was $3-5$ μm.

The spatial distribution of indirect excitons, as inferred from the PL pattern, undergoes a striking transformation as a function of photoexcitation power, P_{ex}. While at low P_{ex} the indirect excitons are observed only within the excitation spot, at high P_{ex} the most prominent feature in the PL pattern is a bright ring concentric with the laser spot and separated from it by an annular dark region. The radius of the ring increases with P_{ex} [15] [Fig. 1].

How can excitons appear so far away from the excitation? The excitons can, in principle, travel in a dark state after having been excited, until slowed down to a velocity below photon emission threshold, where they can decay radiatively [18]. This mechanism can account for the inner ring of smaller radius up to tens of microns observed around the excitation spot [15]. However, within this framework, a number of qualitative features of the external ring appear to be difficult to explain. In particular, why is it so sharp (Fig. 1), why does the ring radius change with gate voltage, and why do rings produced by several excitation spots interact before overlapping?

To that end, we are led to assume that the excitons *are generated* at the ring. Most of the hot electrons and holes, created by the off-resonance excitation [15], cool down and form excitons giving rise to PL observed within or near the laser spot. However, charge neutrality of the carriers excited in the CQW by an off-resonance laser excitation is generally violated mainly due to electrons and holes having a different collection efficiency to the CQW [19]. Overall charge neutrality in the sample is maintained by opposite charge accumulating in the doped regions outside CQW. We note parenthetically that the sign of carrier imbalance cannot be deduced from first principles. We speculate that the current through CQWs from n-doped GaAs layers [Fig. 1(d)] creates an electron gas in the CQW, while excess holes are photogenerated in the laser excitation spot. However, nothing in the discussion and conclusions below will be affected if electrons are replaced by holes and vice versa.

The holes created at the excitation spot diffuse out and bind with electrons, forming indirect excitons. This process depletes electrons in the vicinity of the laser spot, creating an essentially electron-free and hole-rich region, which allows holes to travel a relatively large distance without encountering electrons. At the same time, a spatial nonuniformity in the electron distribution accumulates, causing a counterflow of electrons towards the laser spot. A sharp interface between the hole-rich region and the outer electron-rich area forms [Fig. 1(c)], since a carrier crossing into a minority region binds rapidly with an opposite carrier to form an exciton. (Recently, a possible relationship between the charge imbalance of photoexcited carriers and PL ring patterns has been discussed informally by Igor Kukushkin and David Snoke.)

The mechanism of charge transport can be explored within a simple model in which electrons and holes move in the CQW plane, each species in its own quantum well, governed by the coupled diffusion equations

$$\begin{aligned} \dot{n} &= D\Delta n - wnp + J(r), \\ \dot{p} &= D'\Delta p - wnp + J'(r), \end{aligned} \tag{1}$$

with $n(r)$ and $p(r)$ the electron and hole concentration, D, D' the diffusion constants, and w the rate at which an electron and hole bind to form an exciton. The source term for holes is localized at the excitation spot, $J'(r) = P_{ex}\delta(r)$, while the electron source is spread out over the entire plane, $J(r) = I(r) - a(r)n(r)$, with $I(r)$ and $a(r)n(r)$ the currents in and out of the CQW. The stationary solution of Eqs. (1), with spatially independent parameters I and a, displayed in Fig. 1(c), indeed shows a structure of two regions dominated by electrons and holes, and separated by a sharp interface where the exciton density $n_X \propto np$ is peaked.

To find the ring radius R, we note that the nonlinear term wnp in (1) is small away from the n-p interface, which warrants solving linear equations for $p(r)$ and $n(r)$ separately in each region, and matching the solutions at the boundary. Solving the 2D Poisson equation, the hole concentration within R is set by $p_{r<R} = (1/2\pi)P_{ex} \times \ln(R/r)$, while the electron concentration $n_{r>R}$ is given by

$$n_0 - n(r) = \int \frac{Ae^{i\mathbf{kr}}d^2k}{\mathbf{k}^2 + \lambda^{-2}} \simeq \begin{cases} 2\pi A \ln(\lambda/r), & r \ll \lambda, \\ 0, & r \gg \lambda, \end{cases} \tag{2}$$

with $n_0 = I/a$ the electron density in the absence of excitation, and $\lambda = (D/a)^{1/2}$ the depletion length, here assumed to be large. After the constant A is fixed by the condition $n_{r=R} = 0$, the ring radius can be found from the balance between the radial hole flux and electron counterflow at the interface $r = R$, yielding

$$R = \lambda \exp(-2\pi D n_0/D' P_{\rm ex}), \tag{3}$$

increasing with $P_{\rm ex}$, as in the experiment [Figs. 1(a) and 1(b)].

The density variation across the p-n interface is described by a 1D system of stationary equations, $Dn'' = wnp$, $D'p'' = wnp$, with the boundary conditions $Dn_{x\to+\infty} = cx$, $n_{x\to-\infty} = 0$, where c is particle flux normal to the interface and, by symmetry, $D'p(x) = Dn(-x)$. The interface width scales as $(DD'/wc)^{1/3}$.

The ring can be externally controlled by gate voltage: reducing the voltage across the structure from $V_g = 1.3$ V to $V_g = 1.262$ V makes the ring expand from $R \simeq 180$ to $R \simeq 300$ μm (at $P_{\rm ex} = 1.4$ mW), see Fig. 2 in Ref. [20]. Ring expansion with reducing V_g is consistent with Eq. (3) since a reduction of transverse electric field, and hence of the current $I(r)$, depletes electrons in the CQWs, while holes in the inner region remain practically unaffected.

Experiments with two rings created by spatially separated laser spots [Figs. 2(a)–2(d)] reveal the most intriguing prediction of the transport model: the carrier distribution is strongly perturbed not only inside, but also outside the ring. As the spots are brought closer, the rings attract one another, deform, and then open towards each other [Figs. 2(a)–2(c)]. This happens well before the rings coalesce into a common oval-shaped ring [Fig. 2(d)], suggesting the existence of "dark matter" outside the rings that mediates the interaction. In the transport model, which readily accounts for the attraction [Figs. 2(e)–2(g)], this dark matter is just the electron flow outside each ring which is perturbed by the presence of another ring. Electrons in the area between the rings are depleted more strongly than at the same radial distance in other directions, which shifts the balance of carrier fluxes to the hole side. As a result, the electron-hole interface moves further out between the rings.

The configuration of the electron-hole interface in a stationary state can be easily obtained by noting that the time-independent Eqs. (1) yield the Poisson equation $\Delta\Phi = J_{\rm tot} \equiv J' - J$ for the linear combination of electron and hole densities $\Phi = Dn - D'p$. The solution

$$\Phi(\mathbf{r}) = -\frac{1}{2\pi}\int \ln|\mathbf{r} - \mathbf{r}'| J_{\rm tot}(\mathbf{r}') d^2 r' \tag{4}$$

describes hole density in the region $\Phi > 0$ and electron density in the region $\Phi < 0$. The interface is thus given by the contour line $\Phi = 0$. In particular, two hole sources of equal strength at $\mathbf{r} = \mathbf{r}_{1,2}$ give a family of Bernoulli lemniscata $|\mathbf{r} - \mathbf{r}_1| \times |\mathbf{r} - \mathbf{r}_2| = \text{const}$ [Figs. 2(e)–2(g)].

By defocusing the source and illuminating a large area (Fig. 3), a striking new feature emerges. In the indirect exciton PL pattern, around the localized spots, small

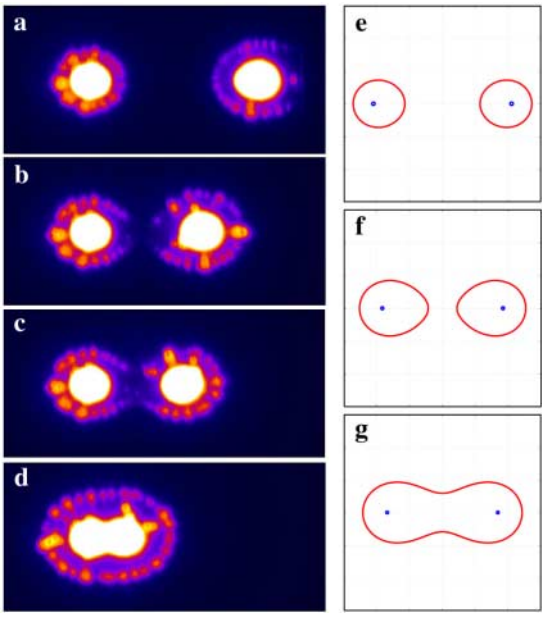

FIG. 2 (color online). Pattern of indirect exciton PL for two sources at $T = 380$ mK, $V_g = 1.24$ V, and $P_{\rm ex} = 230$ μW per beam for different separations (a)–(d) between the excitation spots. The area of view is 520×240 μm; (e)–(g) theoretical prediction for the electron-hole interface evolution at decreasing distance between the two point sources (the scales are in a.u.). Note the ring attraction in (b),(c),(f).

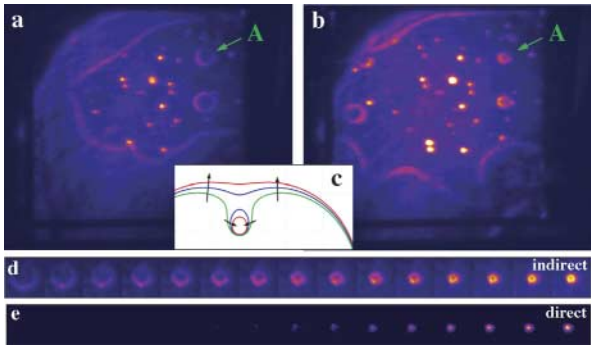

FIG. 3 (color online). Shrinkage of exciton rings to localized bright spots at nearly homogeneous excitation: Spatial PL pattern for indirect excitons at $T = 1.8$ K, $V_g = 1.15$ V, and (a) $P_{\rm ex} = 390$ μW and (b) $P_{\rm ex} = 600$ μW. With (a),(b), the area of view is 690×590 μm. (c) Theoretical electron-hole interface for a point source of holes and a weaker point source of electrons. Arrows show interface displacement at increasing hole number. Note the ring shrinking around electron source. The shrinkage of ring A (a),(b) of indirect excitons is detailed in (d) for $T = 380$ mK, $V_g = 1.155$ V, and $P_{\rm ex} = 77$–160 μW (from left to right) with defocused excitation spot maximum moved to a location directly below ring A. With (d),(e), the area of view is 67×67 μm for each image. Ring shrinkage is accompanied by the onset of the direct exciton emission (e) indicating hot cores at the center of the collapsed rings.

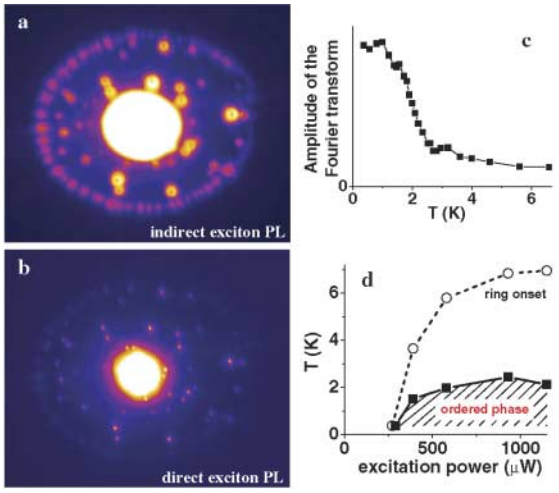

FIG. 4 (color online). Fragmented ring and localized spots in the (a) indirect and (b) direct exciton PL image. The area of view is 410×340 μm. Note that the hot cores with high energy direct excitons, present in the localized spots, are absent in the ring fragments. (c) Exciton density Fourier transform peak height at the fragmentation period vanishes continuously at a critical temperature. (d) The phase diagram of the states of the external ring. The phase boundary of the modulated state observed at the lowest experimental temperatures (solid line) along with the ring onset region (dashed line) are marked.

rings appear which mirror the behavior of the outer ring. However, the rings *shrink* at increasing laser power, indicating that electron-hole contrast here is inverted. This suggests that the spots reflect pinholes in the CQW barriers, each representing a localized source of electrons embedded in the hole-rich inner area. A model with a bright hole source and a weaker electron source [Eqs. (1) and (4)] shows the same qualitative behavior [Fig. 3(c)]. Increasing hole flux (via P_{ex}), as soon as the electron source is enveloped by the hole-rich area, a ring forms around it and then starts to shrink.

The most surprising feature of the PL pattern is ring fragmentation into aggregates forming a highly regular, periodic array over macroscopic lengths of up to ca. 1 mm (Figs. 1–4). These aggregates are clearly distinct from the localized bright spots originating from the pinholes: In contrast to the latter, the aggregates move in concert with the ring when the position of the source is adjusted. Moreover, in contrast to the spots, the aggregates are *cold*: they do not contain direct excitons [Figs. 4(a) and 4(b)].

The conditions in the ring are optimal for the formation of a very cold exciton gas: the excitons in the ring are formed from well-thermalized carriers and, more importantly, due to extremely long lifetimes of indirect excitons the binding energy released at exciton formation has little effect on their temperature. Cold exciton temperatures in the ring allow observation of the ordering which appears abruptly at temperature below ca. 2 K. The phase diagram, obtained from PL distribution along the ring [Fig. 4(c)], is presented in Fig. 4(d).

The exciton ring instability and the formation of the spatially modulated state has not been anticipated. The temperature dependence (Fig. 4) indicates that the observed ordering is a low-temperature phenomenon. However, the origin of this state is, at present, unclear.

We thank A. L. Ivanov, L. V. Keldysh, I. V. Kukushkin, D.-H. Lee, and P. B. Littlewood for valuable discussions. Communications on the theory of PL patterns based on exciton transport by A. L. Ivanov are greatly appreciated. This work was supported by the Office of Basic Energy Sciences, U.S. Department of Energy under Contract No. DE-AC03-76SF00098 and by RFBR. L. L. acknowledges support from "Non-Equilibrium Summer Institute at Los Alamos" and the MRSEC Program of the NSF under Grant No. DMR 98-08941.

[1] L. V. Keldysh and A. N. Kozlov, Sov. Phys. JETP **27**, 521 (1968).
[2] L. V. Keldysh and Yu.V. Kopaev, Sov. Phys. Solid State **6**, 2219 (1965).
[3] D. Yoshioka and A. H. MacDonald, J. Phys. Soc. Jpn. **59**, 4211 (1990).
[4] X. M. Chen and J. J. Quinn, Phys. Rev. Lett. **67**, 895 (1991).
[5] Yu.E. Lozovik and V. I. Yudson, Sov. Phys. JETP **44**, 389 (1976).
[6] A. L. Ivanov, P. B. Littlewood, and H. Haug, Phys. Rev. B **59**, 5032 (1999).
[7] X. Zhu, P. B. Littlewood, M. S. Hybertsen, and T. M. Rice, Phys. Rev. Lett. **74**, 1633 (1995).
[8] A. L. Ivanov, Europhys. Lett. **59**, 586 (2002).
[9] T. Fukuzawa, E. E. Mendez, and J. M. Hong, Phys. Rev. Lett. **64**, 3066 (1990).
[10] L. V. Butov, A. Zrenner, G. Abstreiter, G. Böhm, and G. Weimann, Phys. Rev. Lett. **73**, 304 (1994).
[11] L. V. Butov and A. I. Filin, Phys. Rev. B **58**, 1980 (1998).
[12] A. Parlangeli, P. C. M. Christianen, J. C. Maan, I. V. Tokatly, C. B. Soerensen, and P. E. Lindelof, Phys. Rev. B **62**, 15 323 (2000).
[13] L. V. Butov, A. L. Ivanov, A. Imamoglu, P. B. Littlewood, A. A. Shashkin, V. T. Dolgopolov, K. L. Campman, and A. C. Gossard, Phys. Rev. Lett. **86**, 5608 (2001).
[14] A. V. Larionov, V. B. Timofeev, P. A. Ni, S. V. Dubonos, I. Hvam, and K. Soerensen, JETP Lett. **75**, 570 (2002).
[15] L. V. Butov, A. C. Gossard, and D. S. Chemla, cond-mat/0204482; Nature (London) **418**, 751 (2002).
[16] D. Snoke, S. Denev, Y. Liu, L. Pfeiffer, and K. West, Nature (London) **418**, 754 (2002).
[17] D. Snoke, Science **298**, 1368 (2002).
[18] J. Feldmann, G. Peter, E. O. Göbel, P. Dawson, K. Moore, C. Foxon, and R. J. Elliott, Phys. Rev. Lett. **59**, 2337 (1987).
[19] A. Zrenner, J. M. Worlock, L. T. Florez, J. P. Harbison, and S. A. Lyon, Appl. Phys. Lett. **56**, 1763 (1990).
[20] L. V. Butov, L. S. Levitov, A. V. Mintsev, B. D. Simons, A. C. Gossard, and D. S. Chemla, cond-mat/0308117.